ON REALIZATION OF CINEMA HALL FIRE SIMULATION USING FIRE DYNAMICS SIMULATOR

Lukas VALASEK, Jan GLASA

Institute of Informatics
Slovak Academy of Sciences
Dubravska cesta 9
845 07 Bratislava, Slovakia
e-mail: {lukas.valasek, jan.glasa}@savba.sk

Abstract. Currently known fire models are capable to describe fire dynamics in complex environments incorporating a wide variety of fire-related physical and chemical phenomena and utilizing large computational power of contemporary computers. In this paper, some issues related to realization of the simulation of fire in a cinema hall with sloping floor and curved ceiling furnished by upholstered seats modelled by FDS (Fire Dynamics Simulator) are discussed. The paper concentrates particularly on the impact of a computational meshes choice on resolving flow field and turbulence in the simulation and indicates problems related to parallelization of the calculation illustrated comparing sequential and parallel MPI calculation using 6 CPU cores. Results of the simulation described and their discussion demonstrate the ability of FDS simulation to capture main tendencies of smoke spread and to forecast the related safety risks realistically.

Keywords: Fire modelling, simulation, parallel calculation, FDS, MPI

Mathematics Subject Classification 2010: 68U20, 65Y05

1 INTRODUCTION

Computer simulation of fire dynamics in buildings is a means which can improve the fire safety and structural resistance already in the building design phase. It allows for testing of fire detection, ventilation, compartmentation, egress, suppression tactics as well as a response of the fire management to fire. Future fire-fighting strategies

shall not need to rely mainly on the experience and intuition of commanding officers in duty. It would be a great advantage if the decisions could be based on a prior knowledge of fire development, structural response, and short- or medium-term forecasts. Such approach allows for preparation of more efficient strategies in advance, consequently saving lives and reducing damage and costs and also improving the safety of fire fighters [15].

Rapid growth of the performance of contemporary computers and advances in the CFD (Computational Fluid Dynamics) theory have led to development of fire simulators which appear to be powerful enough to simulate many practical problems such as compartment fires and outdoor fires including pyrolysis phenomena and flashover in an enclosure [3, 45]. Current fire models are now capable of describing fire in complex environments incorporating a wide variety of fire-related physical and chemical phenomena. Early fire models were specifically designed to study fire impact on buildings. These models were based on empirical correlations which provided estimates of plumes, compartment temperatures, heat fluxes and smoke concentrations. In the seventies these correlations were incorporated into *zone models*, where a physical space has been split in two spatially relatively homogeneous zones; a hot upper layer and a colder lower layer. A theoretical background of the zone models includes conservation laws of mass and energy related to layer, supplemented by additional models describing the fire plumes, gas flows through vents, radiative and convective heat transfer, and pyrolysis of solid substances [5, 16, 29]. Physical and computational simplicity of the zone models have led to their widespread use especially for analysis of compartment fire scenarios in which the 2-layer assumption is valid and a detailed spatial resolution is not required [22]. In the nineties, CFD-based *field models* were introduced. These models are based on the Reynolds-averaged form of the Navier-Stokes equations and they were developed as a time-averaged approximation to the conservation equations of the fluid dynamics describing transfer of mass, momentum and energy by gas flows induced by fire. Simplified conservation equations suitable for modelling low-speed gas flows driven by chemical heat release and buoyancy forces, that are referred to as the low Mach number combustion equations [30, 26], have been widely adopted by the combustion research community. Equations are capable of being solved numerically in the efficient way using 3D rectilinear computational meshes consisting of a large number of rectangular cells. Within each cell, a gas velocity, a temperature, and other relevant quantities are assumed to be uniform, varying only over time. However, the simulation accuracy is significantly affected by the mesh resolution. The number of cells incorporated into the simulation is limited by the available computing power (there are now several millions of cells per single processor; each cell requires 1 kB of RAM).

At present, several fire simulators are available in which CFD-based fire field models have been implemented. We have tested the FDS (Fire Dynamics Simulator) system for simulation of car fires [10], tunnel fires [6, 7, 38, 41], and car park fires [42, 43, 2]. Results of these simulations indicate that FDS is able to cap-

ture fire behaviour realistically. In the literature, several papers have dealt with the applicability of FDS for simulation of fires in various structures with higher density of visitors, for instance in a theatre [40, 44], supermarket [17], compartment [18, 45, 34, 46, 4] or building [31, 13, 14]. It has been observed that the FDS simulations were capable to describe reliably a complex dynamics of fire in such structures. Recently, we used FDS to illustrate the course of fire in a small cinema hall with a sloping floor and a curved ceiling furnished by 108 upholstered chairs [36, 37, 8, 9]. In the research we used default dominant reaction to describe the fire chemistry and the fire source given by HRRPUA (heat release rate per unit area) in the corresponding SURF line.

In this study we describe the dynamics of a 1-minute fire in a similar cinema hall with a sloping floor and a curved ceiling furnished by 108 upholstered chairs, focusing on realization of the simulation, particularly on some specific issues related to its sequential and parallel calculation. The fire chemistry is specified more accurately by setting HEAT_OF_REACTION along with other thermal parameters for upholstery material on the corresponding MATL lines. In this case the burning rate of a fuel depends on the net heat feedback to the surface (in both cases a mixture fraction combustion model is used). As burning of upholstered chairs is known to release extremely toxic gases [28], our analysis is focused more on potential threats of smoke spread than on those of temperature increase. Material parameters of upholstery considered here have been validated by full-scale fire experiments including upholstered chairs and by FDS simulation and determined by laboratory measurements [11]. The paper particularly concentrates on proper choice of computational mesh/meshes for given simulation in order to sufficiently resolve the fire dynamics and flow field in the given structure and illustrates potential differences in simulation results comparing efficiency and accuracy of realised sequential and parallel calculations.

The paper has a following structure. In Section 2, a brief physical and mathematical background of FDS is summarised. Section 3 describes the cinema hall considered, fire scenario and their FDS representation. Section 4 includes a study on realization of the simulation including the simulation results analysis, pointing out to some problems related to the choice of computational meshes and the computation parallelization. In Section 5, main conclusions and some challenges for future research are discussed.

2 COMPUTER SIMULATION OF FIRE BY FDS

FDS (Fire Dynamics Simulator) [21, 20] is an open source CFD-based fire field model developed by NIST (National Institute of Standards and Technology, U.S. Department of Commerce) in cooperation with VTT (Technical Research Centre of Finland). FDS numerically solves a form of the Navier-Stokes equations for low-speed thermally driven flows with the emphasis on transfer of smoke and heat from the fire. The set of governing fluid dynamics equations for multi-component mixture

of ideal gases in the presence of energy and mass sources is defined in the following form [21]:

$$\frac{\partial \rho}{\partial t} + \nabla.\rho\mathbf{u} = \dot{m}_b''',\tag{1}$$

$$\frac{\partial}{\partial t}(\rho Y_\alpha) + \nabla.\rho Y_\alpha\mathbf{u} = \nabla.\rho D_\alpha\nabla Y_\alpha + \dot{m}_\alpha''' + \dot{m}_{b,\alpha}''',\tag{2}$$

$$\frac{\partial}{\partial t}(\rho\mathbf{u}) + \nabla.\rho\mathbf{u}\mathbf{u} + \nabla p = \rho\mathbf{g} + \mathbf{f}_b + \nabla.\tau_{ij},\tag{3}$$

$$\frac{\partial}{\partial t}(\rho h_s) + \nabla.\rho h_s\mathbf{u} = \frac{Dp}{Dt} + \dot{q}''' - \dot{q}_b''' - \nabla.\dot{\mathbf{q}}'' + \varepsilon,\tag{4}$$

$$p = \frac{\rho R T}{\bar{W}}\tag{5}$$

where ρ is the density, $\mathbf{u} = (u, v, w)^T$ is the velocity vector, $\dot{m}_b''' = \sum_\alpha \dot{m}_{b,\alpha}'''$ is the production rate of species by evaporating droplets or particles, Y_α, D_α, and $m_{b,\alpha}'''$ are the mass fraction, diffusion coefficient and mass production rate of αth species per unit volume, respectively, $\mathbf{g}$ is the acceleration of gravity, p is the pressure, $\mathbf{f}_b$ is the external force vector, $\tau_{\mathbf{i,j}}$ is the viscous stress tensor, h_s is the sensible enthalpy, $D()/Dt = \frac{\partial()}{\partial t} + \mathbf{u}.\nabla()$, $\dot{q}'''$ is the heat release rate per unit volume from a chemical reaction, $\dot{q}_b'''$ is the energy transferred to the evaporating droplets, $\dot{\mathbf{q}}''$ represents the conductive and radiative heat fluxes, ε is the rate of kinetic to thermal energy transform, R is the universal gas constant, T is the temperature, and $\bar{W}$ is the molecular weight of the gas mixture. Equations (2) represent the mass conservation equation (1) expressed in terms of the individual gaseous species. Summing the Equations (2) over all species yields the Equation (1). The system (1)–(5) is a system of six equations (the equation of mass, species, momentum and energy conservation, and the state equation) with six unknowns: the density ρ, three components of velocity $\mathbf{u}$, temperature T, and pressure p, which are functions of three spatial dimensions and time. The Equations (1)–(5) are modified and simplified, and then discretized and numerically solved on 3D orthogonal meshes. Applying the divergence operator on the momentum equation (3) written in the form $\frac{\partial \mathbf{u}}{\partial t} + \mathbf{F} + \nabla H = 0$, where H is the total pressure divided by the density, the equation $\nabla^2 H = -\frac{\partial}{\partial t}(\nabla.\mathbf{u}) - \nabla.\mathbf{F}$ of the Poisson type can be obtained which is referred to as pressure equation. FDS uses the simplified low Mach number governing equations, where sound waves are filtered out in order to correspond to flows typical for fires (10–20 m/s). The core numerical scheme used in FDS is an explicit predictor-corrector finite difference scheme, which is second-order accurate in time and in space. The flow variables are updated in time using an explicit second-order Runge-Kutta scheme. The pressure equation is capable of being efficiently numerically solved by a fast, direct solver optimized for uniform meshes, based on FFT (Fast Fourier Transform) [33]. The use of FFT involves some additional limitations to chosen underlying computational meshes. Since the accuracy of resolving flow fields in simulation is dependent on resolution

of the chosen computational meshes, we discuss the mesh sensitivity study in the paper as well.

Turbulence is modelled by the Smagorinsky form of LES (Large Eddy Simulation) in most applications [23, 27]. In this paper we show some a posteriori metrics of quality of chosen computational meshes used in simulation in order to illustrate the impact of mesh resolution on resolving velocity and scalar fields calculated by LES. In FDS, the Direct Numerical Simulation (DNS) is also available for applications where the used numerical grid is fine enough.

Combustion modelling is based on the mixture fraction concept, where the mixture fraction is a conserved scalar quantity defined as the fraction of gas at a given point of the flow field that originates as fuel. Several optional schemes are available for combustion predictions in under-ventilated compartments. The mass fractions of all the major reactants and products can be derived from the mixture fractions using relations based on simplified analysis and measurement. The simplified approach to the chemistry of fire still involves at least six primitive gas species (fuel, O_2, CO_2, H_2O, CO, N_2) and soot. Since combustion is typically considered as a mixing-controlled single-step reaction of fuel and oxygen, two transport equations (for the fuel and for the products) need to be solved explicitly. The conversion of species from one to the other can be then represented as a matrix multiplication because the mass fractions of air, fuel and products are linearly related to the primitive species mass fractions (for more details see [22, 20]). Because of increasing computational complexity of calculation, the number of fuels, and the number of reactions is usually limited to one, and one or two, respectively. In the model it is also supposed that the reaction may not proceed due to lack of sufficient oxygen in the incoming air, as when a fire in a closed compartment extinguishes itself.

Radiative heat transport is modelled using the Finite Volumes Method (FVM) solving the radiation transport equation for a gray gas. Using approximately 100 discrete angles which are updated over multiple time steps, the finite volume solver requires about 20 % of the total CPU time of calculation. Absorption and scattering of thermal radiation by water droplets in applications involving sprinklers are derived from Mie theory. However, scattering from the gaseous species and soot is not included in the model. For all solid surfaces, thermal boundary conditions and information about the burning behaviour of the materials are assigned. Heat and mass transfer to and from solid surfaces is handled with empirical correlations or computed directly when performing LES or DNS, respectively. Sprinkler sprays may also be modelled in FDS by Lagrangian particles representing a sampling of the water droplets ejected from the sprinkler; activation of heat and smoke detectors is also included.

All input parameters describing a particular scenario are written in a single text file which comprises information about the numerical grid, ambient environment, building geometry, material properties, combustion kinetics, and types and form of output quantities desired by the user. The physical space is split into one or more rectilinear computational meshes to which the geometry of all objects must conform. Nowadays, parallel versions of FDS are available which make it possible to simulate

fires in large areas; however, decomposing large computational spaces is a problem which must be seriously analysed and coupling of the pressure solver across the mesh boundaries in multi-mesh simulations must be tested and verified.

FDS computes the temperature, density, pressure, velocity and chemical composition within each numerical grid cell at each discrete time step, as well as temperature, heat flux, mass loss rate, and other various quantities of solid surfaces. Typical output quantities for the gas phase include gas temperature and velocity, gas species concentration (water vapour, CO_2, CO, N_2), smoke concentration and visibility estimates, pressure, heat release rate per unit volume, mixture fraction, gas density and water droplet mass per unit volume. On solid surfaces, FDS predicts additional quantities associated with the energy balance between gaseous and solid phases, including the surface and interior temperature, radiative and convective heat fluxes, burning rate and water droplet mass per unit area. Global quantities recorded include the total heat release rate (HRR), sprinkler and detector activation times and mass and energy fluxes through openings or solids. The outputs can be visualized in the form of numbers, graphs, tables, pictures and animations by Smokeview, including contour, vector, or surface plots of static and animated data.

FDS has been developed to run on a variety of platforms and operating systems. To utilize all available computing resources effectively seeking to obtain the best performance, FDS supports the configuration of four programming models, such as sequential model, parallel MPI model, multi-threading OpenMP model and hybrid MPI & OpenMP model [41]. The sequential model is designed for running on a single CPU. The parallel MPI model is designed for running on distributed memory systems. To execute FDS as a single parallel job on a distributed memory system, the MPI (Message-Passing Interface) [24] is applied. The main strategy consists in decomposition of the computational domain into multiple meshes and computing of the flow field in each mesh is performed as an individual MPI process; MPI routines handle the transfer of information between these processes. The multi-threading OpenMP model is designed for running on shared memory systems. FDS multi-threading is implemented through the OpenMP library [25], which allows the concurrent execution of multiple threads within the context of a single process. The hybrid MPI & OpenMP model is designed for running on distributed shared memory systems (e.g. clusters), which may include a shared memory between cores within a node, and a distributed memory between nodes. The combination of MPI and OpenMP approaches enables to apply a two-level parallelization. In this paper, the sequential and parallel MPI computing models are used and discussed.

3 FIRE SCENARIO AND CINEMA HALL REPRESENTATION IN FDS

We consider a small cinema consisting of the cinema hall, entrance hall and projection room (Figure 1). The cinema hall consists of a stage with two small stairways,

a sloping floor constructed as a stairway consisting of nine 20 cm high stairs, on each of them a chair row is placed, and the 4.6 m high curved ceiling. The seating area for audience consists of 108 upholstered seats organized in aforementioned 9 rows; 3 rows by 10 chairs, 3 rows by 12 chairs and 3 rows by 14 chairs. The chair rows are numbered in ascending manner from the lowest one upwards and the chairs are numbered in ascending manner from left to right.
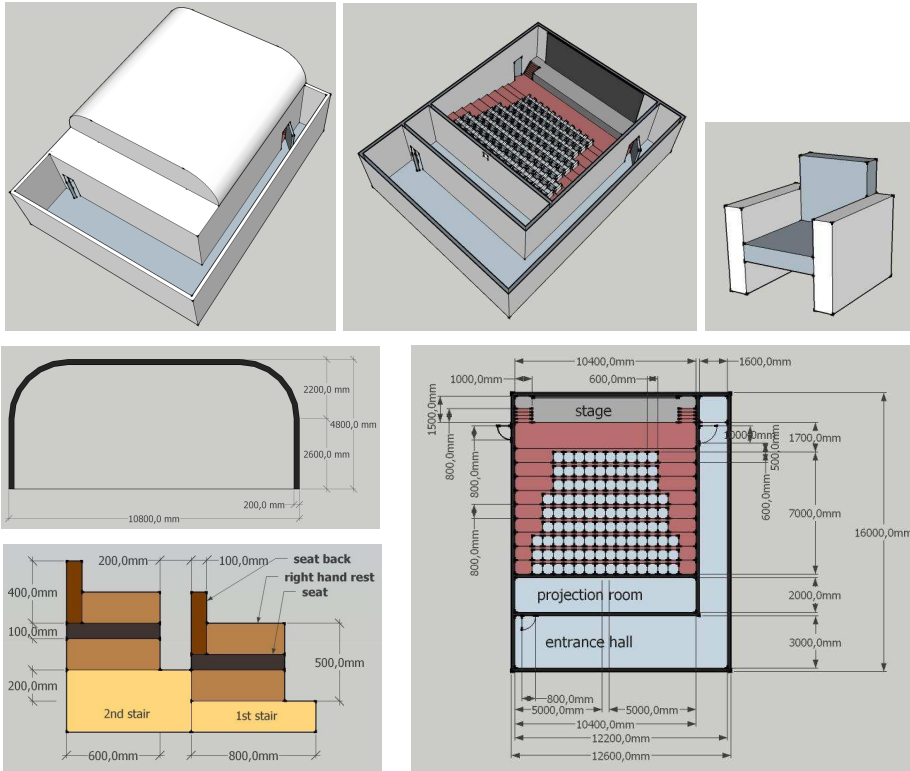

Figure 1. Scheme of the cinema and its interior arrangement and ground plan

We assume a simple fire scenario, in which a fire is initiated at the cinema hall under the left-most chair in the 5th chair row. The fire source of the 110 kW HRR (heat release rate) burning during the whole simulation period placed on the floor under the chair is considered. It was expected that the simulation would confirm that audience would be at risk during the first minute of the fire already, therefore, the simulation duration was set to 60 seconds. It was also assumed that spectators would be more endangered by toxic smoke released from the upholstered chairs fire than by increasing temperature. In order to keep the fire scenario as simple as possible, we assumed that all doors in the cinema hall were closed during the simulation; neglecting the impact of open door on the fire behaviour during the first

minute of the fire. Therefore, we limit the simulated space considered in simulation
to the cinema hall.

The computational domain covers the space of $10.8 \times 10.8 \times 4.8$ m. We consider
a cube computational mesh with the 2.5 cm resolution. Because creating the input
FDS representation of given structure is often laborious and time-consuming, sev-
eral graphical user interfaces have been developed to ease the process. Such tools
enable modelling buildings interactively using ground plans, efficient drawing of rep-
etitious objects, stairways, curved walls and other complex elements of geometry.
For creating geometry of the considered cinema hall we used PyroSim [35] which
was developed as an interactive graphical user interface for FDS by Thunderhead
Engineering in collaboration with The RJA Group, Inc. Figure 2 shows the represen-
tation of the cinema hall created by PyroSim, utilizing its ability to handle efficiently
with the walls drawing, objects grouping, copying and moving groups of objects to
proper positions using the ground plan imported on the background (for more de-
tails see [36, 37]). The use of PyroSim interactive tools allows avoiding laborious and
time-consuming determination of particular coordinates of vertices corresponding to
the individual OBSTRUCTIONs, HOLEs and VENTs representing the cinema hall
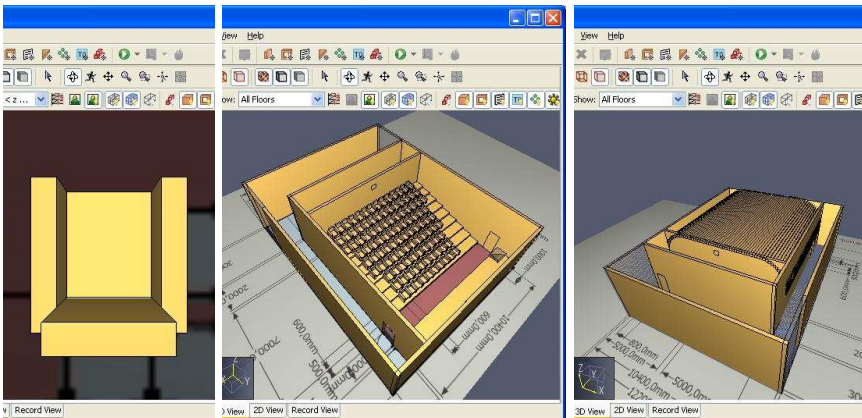and its furnishing (see Table 1).

Figure 2. Input geometry of a chair and the cinema

The initial fire source is represented by a hot 0.4×0.2 m surface with the
$1\,375$ kW/m^2 HRRPUA (heat release rate per unit area) burning during the whole
simulation period. It is placed on the floor under the chair.

We consider three types of materials in simulation: concrete for walls, upholstery
for chairs, and inert material for other surfaces such as the floor, stage, doors,
etc. (see Table 2). The parameters for upholstery were determined by laboratory
measurements and validated by full-scale fire experiments with upholstered chairs
and by FDS simulations [11].

Particular Elements	N_{OBST}	N_{HOLE}	N_{VENT}
Walls	4	–	–
Single chair	4	–	–
Stage with 2 stairways	17	2	–
Sloping floor	9	–	–
Chair rows	432	–	–
Doors	–	–	2
Curved ceiling	65	–	–
Other facilities	–	–	2
The whole structure	**527**	**2**	**4**

Table 1. Cinema hall representation: N_{OBST}, N_{HOLE} and N_{VENT} correspond to the number of OBSTRUCTIONs, HOLEs and VENTs, respectively

Parameter	Concrete	Upholstery
Density kg/m^3	2 280	28.0
Emissivity (–)	0.900	0.900
Specific heat (kJ/kg/K)	1.04	1.70
Heat of combustion (kJ/kg)	–	2.54E04
Conductivity (W/m/K)	1.8000	0.0500
Reference temperature (°C)	–	350
Number of reactions (–)	–	1
Heat of reaction (kJ/kg)	–	1 750.0
Fuel gas yield (kg/kg)	–	1.0
Pre–exponential factor (1/s)	–	1.39E16
Activation energy (kJ/kmol)	–	2.19E05
Carbon atoms in fuel (–)	–	6.3
Hydrogen atoms in fuel (–)	–	7.1
Oxygen atoms in fuel (–)	–	2.1
Nitrogen atoms in fuel (–)	–	1.0
Fraction of soot from the fuel (–)	–	0.1
Phase	Solid	Solid

Table 2. Material properties including reaction parameters for polyurethane

4 REALIZATION OF SIMULATION

In this study we consider two ways of calculation of the fire scenario described above: sequential calculation (denoted by 1M) using a single CPU core and parallel calculation (denoted by 6M) using 6 CPU cores (Figure 3, Table 3). In the first case, the domain is decomposed into a large number of cube volumes (cells) forming a single computational mesh of the 2.5 cm resolution. In the second case, the domain is decomposed into six computational meshes of the same resolution.

Note that corresponding parameters of the meshes used satisfy requirements for FDS computational meshes resulting from the pressure equation implementation
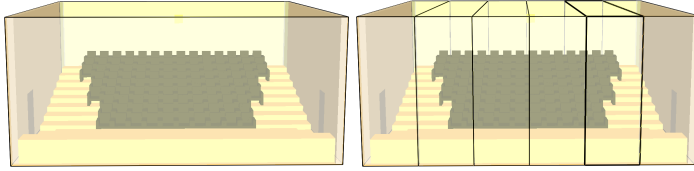
Figure 3. Computational domain decomposition for sequential and parallel calculations

based on FFT. Other issues related to the choice of the meshes for the simulation are discussed in Section 4.2.

Calculation	N_M	N_C	N_{CpM}	N_{CpM}^x	N_{CpM}^y	N_{CpM}^z
1M	1	35 831 808	35 831 808	432	432	192
6M	6	35 831 808	5 971 968	72	432	192

Table 3. Computational domain decomposition for sequential (1M) and parallel (6M) calculations: N_M, N_C, N_{CpM}, N_{CpM}^x, N_{CpM}^y and N_{CpM}^z mean the number of meshes, the number of cells, the number of cells per mesh, the number of cells in x-direction per mesh, the number of cells in y-direction per mesh and the number of cells in z-direction per mesh, respectively

Both calculations were performed on a standard 6-core PC (Intel Core i7-3930K, 3.20 GHz, 64 GB RAM) using the 64-bit 5.5.3 version of FDS for Windows and MPICH2, version 1.2.1.

4.1 Fire Development

In this part, simulation results obtained by the 1M calculation are discussed with the intention of brief description of the simulated fire behaviour and consequences.

The fire development was as follows (Figures 4–6). At the 1st second of fire, flames and dense smoke appeared in front of the chair under which the initial fire source was placed. It corresponds with the fact that there is a semi-closed (opened forwards) space under the chair formed by the floor, chair seat, both side hand rests and the stair on which the 6th chair row is placed. In following seconds, a thin column of smoke moving quickly up to the ceiling was observed which reached the ceiling at the 4th second of fire. After the smoke hit the ceiling, it spread radially under the ceiling. It reached the nearer left and farther right curved part of the ceiling at the 4th and 14th second, respectively. At the 7th and 10th second of fire, the smoke reached the back and front vertical wall of the cinema hall, respectively. The hit of smoke onto the vertical obstacles, whether straight or curved, caused the spread of smoke downwards and turbulent mixing of quick hot gases with cold fresh air. Toxic gas clouds, formed at first in the left back corner and later at the left side part of the cinema hall, can be observed in Figures 4, 5 and 6. Later, the clouds of toxic turbulent gas at the back and under the left curved part of the cinema hall
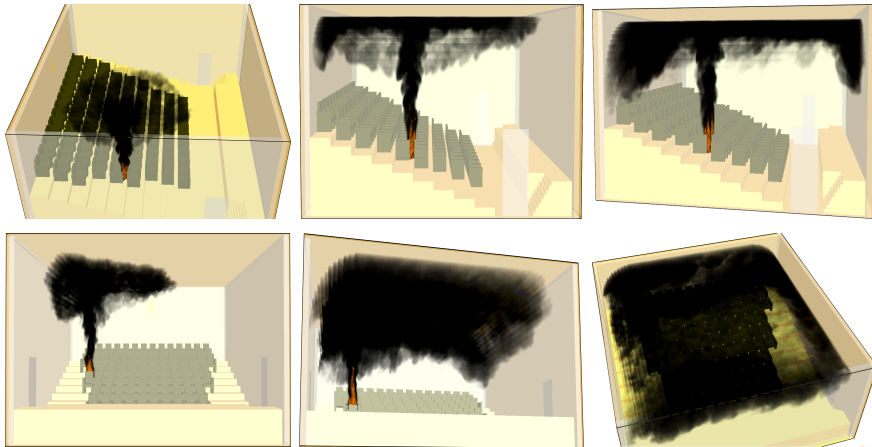
Figure 4. Fire and smoke spread: radial smoke spread under the ceiling at the 6th second (top, left); formation of smoke clouds at the back and front parts of the cinema hall at the 9th and 14th second (top, mid and right); formation of smoke clouds at the back and front parts of the cinema hall at the left and right curved parts of the ceiling at the 9th and 21st second (bottom, left and mid); and increasing toxic clouds at the 22nd second of fire (bottom, right)

increased and the layer of toxic gases under the ceiling thickened. Note that the "flames" visualized in Figures 4 and 5 correspond to fire with the HRRPUA (heat release rate per unit volume) values greater than $200\,\mathrm{kW/m^3}$ and some walls of the cinema hall are made invisible in order to better visualize the flow phenomena which are to be observed. In Figure 6, a sequence of selected slices of the gas temperature and velocity distribution at different times passing through the initial fire source is shown. Note that series of slices of various physical quantities can be animated. Such animations enable to visualize various particular aspects of the fire and smoke spread in time and to describe specific dangerous tendencies of the fire behaviour in particular phases of the fire.

To illustrate the risks to spectators caused by the temperature increase, the point temperatures at eyes levels corresponding to spectators standing in front of and sitting in selected seats in the cinema hall were recorded during the simulation (see Figure 7). Temperature curves corresponding to eye levels of spectators standing in front of the 1st seat in the 1st chair row and in front of the 4th and 7th seats in the 5th chair row do not indicate the risk caused by the temperature increase during the first minute of the fire (Figure 7, left). However, the rapid increase of the temperature at eye level of the spectator standing in front of the 1st seat in the 9th row observed since the 44th second indicates the risk increase. Similarly, no risk is indicated for the spectators sitting on the 1st seat in the 1st chair row, and the 4th and 7th seat in the 5th row (see Figure 7, right). However, the spectator sitting on the 1st seat in the 9th chair row tends to be endangered earlier than the one standing
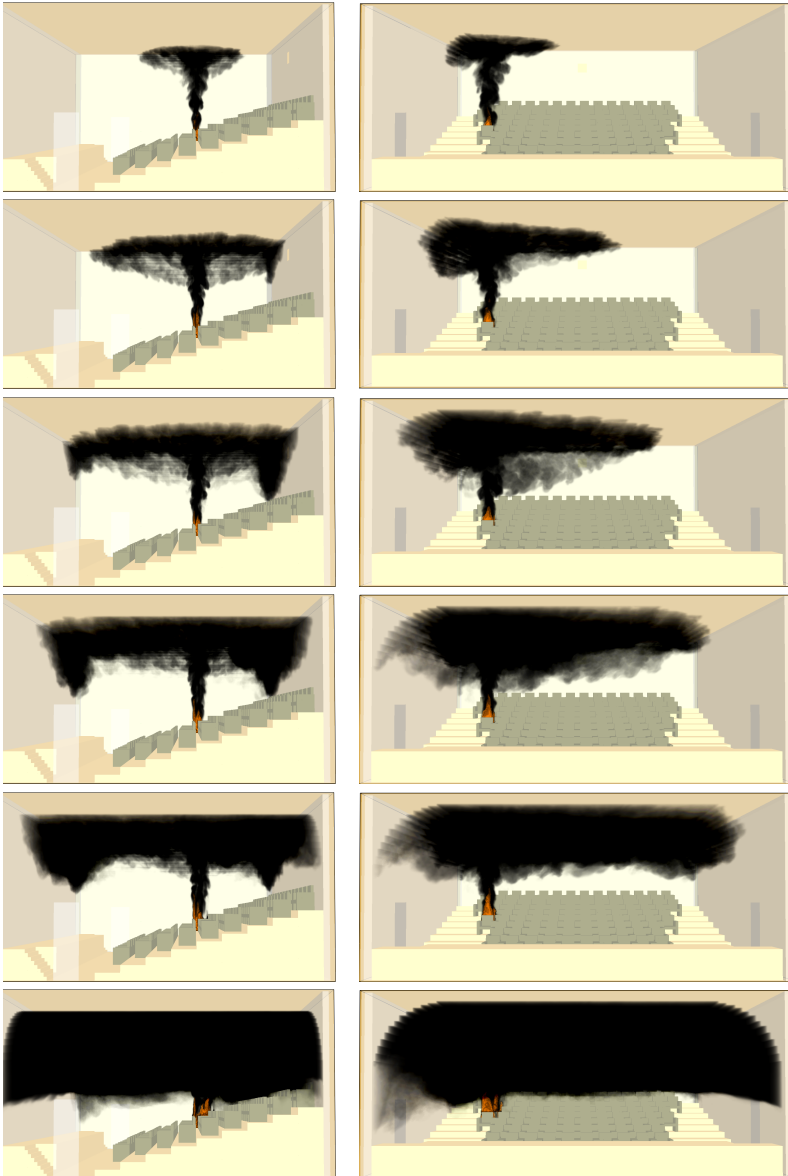
Figure 5. Fire and smoke spread simulation at the 6th, 9th, 12th, 16th, 20th, and 60th second of fire: side view (left) and front view (right)
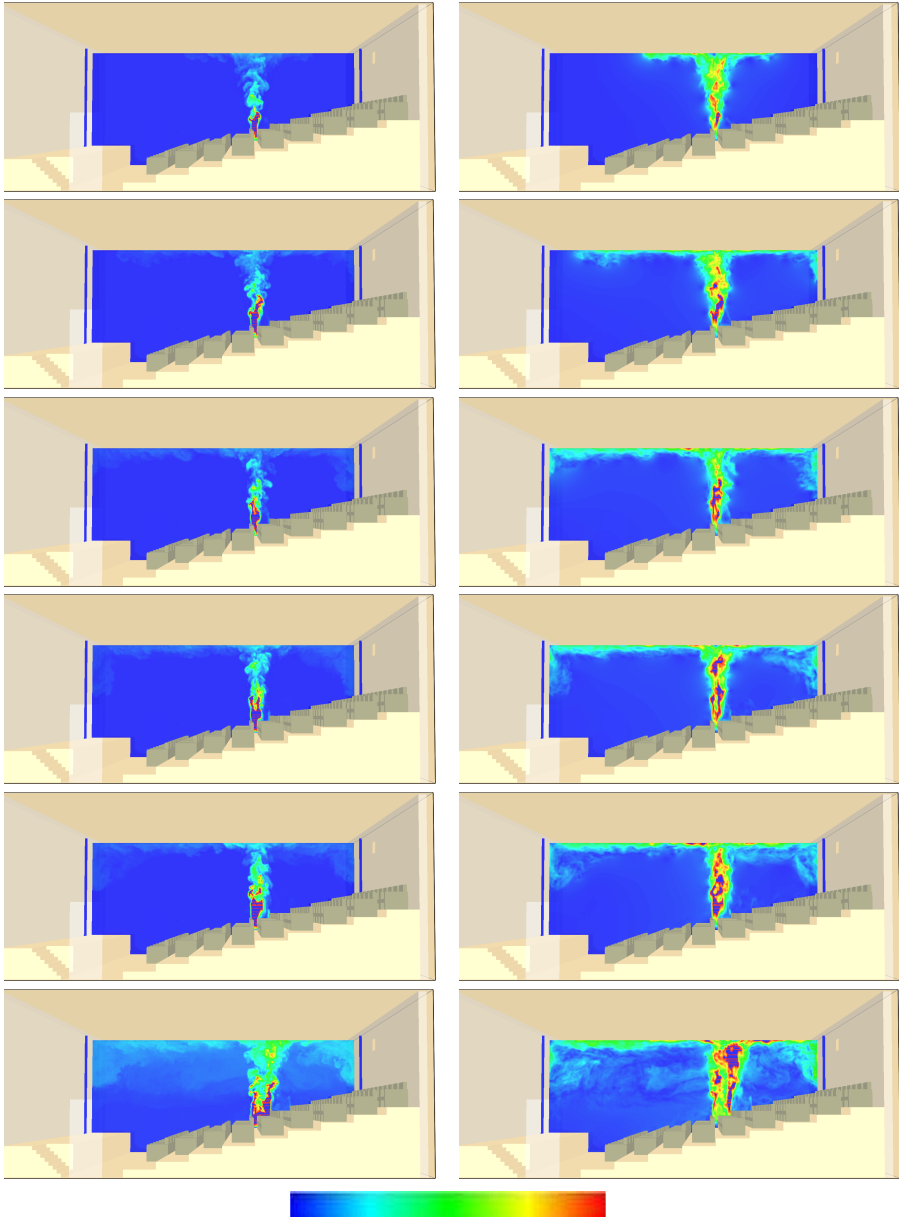
Figure 6. Sequence of slices of the gas temperature (left) and velocity (right) distribution at the 6th, 9th, 12th, 16th, 20th and 60th second of fire; the minimum and maximum values of the gas temperature and velocity in colour scales are $20°$C and $370°$C and $0\,$m/s and $4\,$m/s, respectively
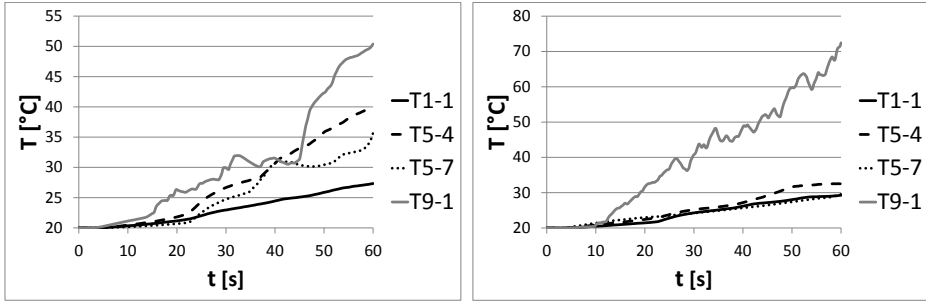
Figure 7. Point temperature curves at eye level of spectators standing in front of (left), or sitting on (right) different seats in the cinema hall: the curves T1-1, T5-4, T5-7, and T9-1 correspond to the 1st seat in the 1st chair row, the 4th seat in the 5th chair row, the 7th seat in the 5th chair row, and the 1st seat in the 9th chair row, respectively. The eye level of standing and sitting spectators is considered at the 1.6 m and 1.2 m height, respectively

in front of the seat because of the characteristic fire spread along the vertical back wall (see also Figures 4, 5 and 6).
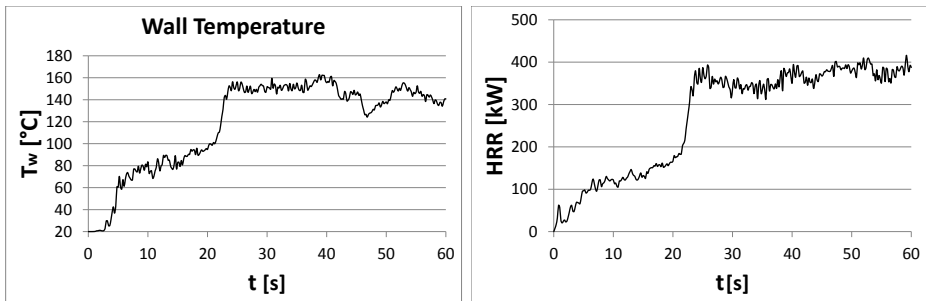

Figure 8. Wall temperature of the ceiling at the points where the temperature reached the highest value and the heat release rate curve

The ceiling surface was heated up to 162.81°C (at the 39th second) during the first 60 seconds of fire (see Figure 8, left). The HRR (heat release rate) curve for the simulated fire is shown in Figure 8 (right). The HRR increase (for the first 21 seconds), rapid acceleration (for 4 seconds), and relatively stable values of HRR (until the end of simulation) can be observed; this corresponds to the fire origin (the spread of fire from the initial fire source onto the lower and front parts of the chair seat), burning of the same surface (not-increasing area), spread of fire from the chair seat onto the front part of seatback and hand rests, and burning of relatively the same area, respectively. The maximal value of the total HRR reached during the first minute of the fire was 416.23 kW (at the 59th second of fire). Note that very
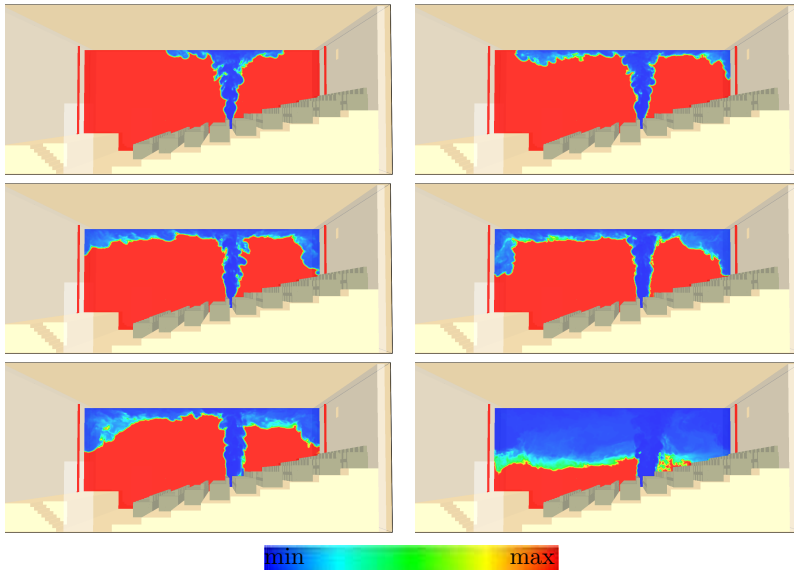
Figure 9. Sequence of soot visibility slices at the 6th, 9th, 12th, 16th, 20th, and 60th second of the fire; the colour scheme values vary from 0 m *(blue) to* 30 m *(red)*

good qualitative correspondence between the wall temperature and HRR curves can be observed in Figure 8.

In Figure 9, we can see a time sequence of the soot visibility slices, selected at the same times as the gas temperature and velocity distribution slices shown in Figure 6.

Figure 10 illustrates the threats caused by an increase of the toxic smoke density to standing or sitting spectators at different places in the cinema hall. Graphs of soot visibility measured at the same points as in Figure 7 are plotted. The visibility curve corresponding to the 1st seat in the 1st row does not indicate any risk in both cases (standing and sitting spectator). In the case of spectators standing in front of the seats, the graphs indicate the danger related to smoke even since the 38th and 34th second for both selected seats in the 5th row and since the 21st second for the 1st seat in the 9th row. However, in the case of sitting spectators the danger appears later and does not last long for those sitting on seats in the 5th row; but it increases much earlier for the 1st seat in the 9th row (see Figure 10 and also Figure 7 and its description).

In Figure 11, a time sequence of selected slices of the gas temperature under the ceiling is illustrated. In accordance with experimental observations and computer simulation of travelling fire in experimental building reported in [13], considerable temperature gradients appeared (see also Figure 6, left). The gas temperature heterogeneity within the cinema hall fire is demonstrated to highlight its potential impact on structural behaviour and safety of people. Due to lack of fire experi-
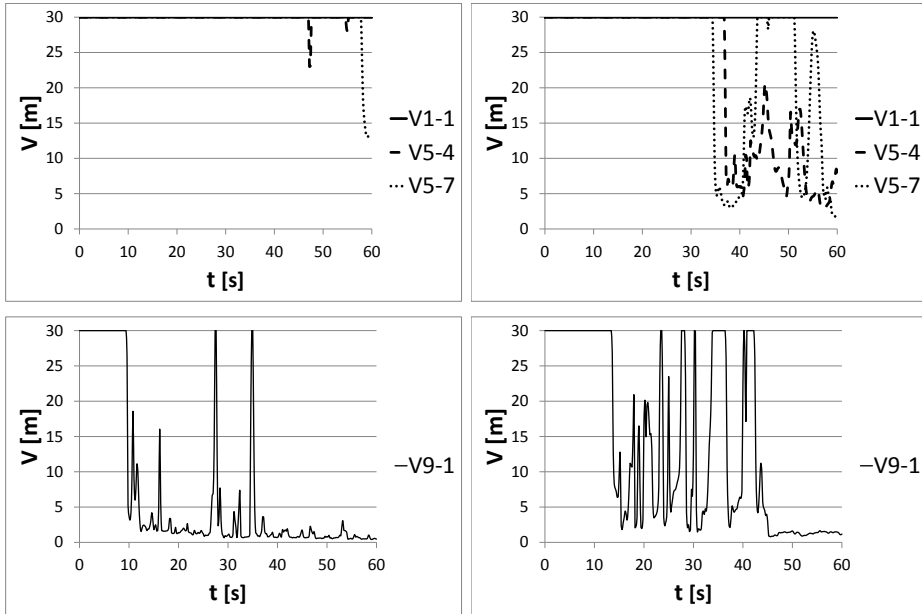
Figure 10. Soot visibility at eye level corresponding to spectators standing in front of (left) or sitting on (right) particular seats in the cinema hall: curves V1-1, V5-4, V5-7 and V9-1 correspond to the 1st seat in the 1st row, the 4th seat in the 5th row, the 7th seat in the 5th row and the 1st seat in the 9th row, respectively

ments in large compartments with real compartment conditions, fire loads, ignition sources and due to limited number of measuring devices, the presence of horizontal temperature heterogeneity has not been investigated yet and is rarely reported in the literature [32]. However, it can result in considerable differences in heat flux affecting the structure and facilities.

4.2 Comments on Some Issues Related to Computational Mesh Choice

The quality of a particular simulation and the total computational time of its calculation are most directly tied to computational mesh resolution. The effect of the mesh resolution on various fire characteristics, such as the flame height, radiative heat fluxes, temperature distribution, etc. has been extensively investigated. It was observed that the measure of how well the flow field is resolved depends on the ratio of the so called characteristic fire diameter in given scenario to the size of a grid cell. It is defined as a non-dimensional expression D^*/dx where D^* is the characteristic fire diameter [20]

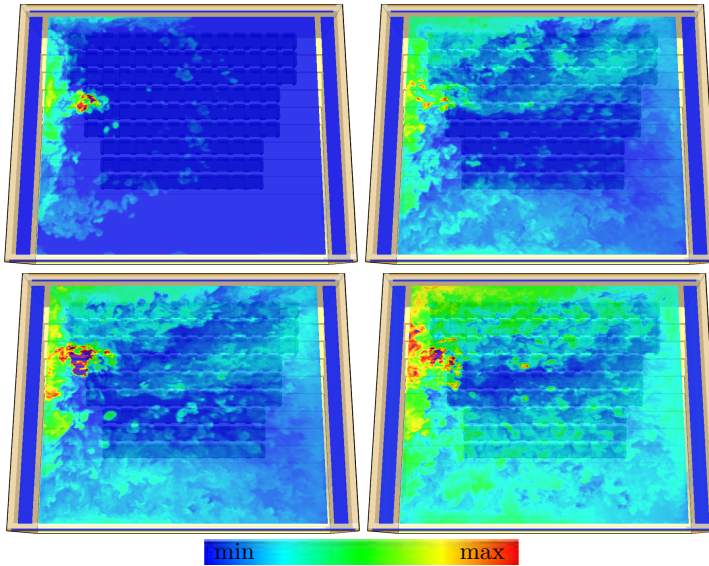$$D^* = \left(\frac{\dot{Q}}{\rho_\infty c_p T_\infty \sqrt{g}} \right)^{2/5},$$

Figure 11. Temperature inhomogeneity under the ceiling: gas temperature of level of 50 cm under the ceiling at the 10th, 22nd, 24th and 29th second of fire; the colour scheme values vary from 20°C (blue) to 95°C (red)

$\dot{Q}$ is the heat release rate, ρ_∞ is the density, c_p is the specific heat, T_∞ is the ambient temperature, g is the gravity and dx is the nominal size of a mesh cell. The ratio D^*/dx can be thought of as the number of computational cells spanning the characteristic diameter of fire. The more cells a fire is spanned by, the better the resolution of the calculation is. The mesh resolution must be specified carefully in order to resolve the flow field calculated in the simulation sufficiently. This measure was used in the study [12] for several types of fire in a nuclear power plant, where the values of the measure greater than 16 indicate that the flow field in simulations is well resolved and the used computational mesh can be considered as "fine".

To choose the proper mesh resolution for the intended simulations, we performed in advace the so called mesh sensitivity study [21]. We realized 5 auxiliary simulations with parameters corresponding to the intended cinema hall fire simulation. In these simulations we used the same fire source, the same geometry of the area and the same type of upholstered chairs. The computational domain with the dimensions of $4.0 \times 4.0 \times 4.8$ m included the corresponding parts of 5 chair rows with 15 seats and the corresponding part of the curved ceiling of the considered cinema hall (Figure 12). The used material properties and other input parameters were the same as in the intended simulation. We considered a shorter duration of fire (20 seconds). Therefore, we set the material conditions of concrete on side boundaries of the computational domain to avoid disproportional losses of
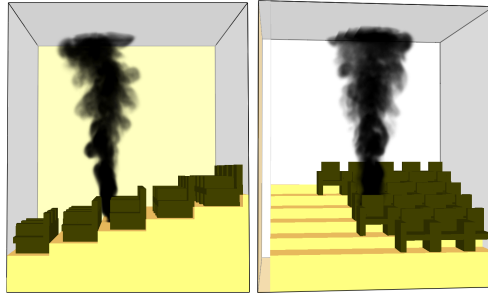
Figure 12. Auxiliary simulation at the 4th second (2.5 cm mesh resolution case)

heat caused by heat leakage through boundaries. Thus we realized 5 simulations using cube computational meshes with the 2, 2.5, 3.$\bar{3}$, 5 and 10 cm mesh resolutions.

In order to analyse the impact of the computational mesh resolution on resolving flow field calculated in a particular simulation, we analysed the HRR values corresponding to all calculations. It can be observed in Figure 13 that the calculated values of HRR corresponding to the 2 and 2.5 cm mesh resolutions are very closed, which indicates that the corresponding meshes could be considered to be sufficiently fine. HRR curves corresponding to the 3.$\bar{3}$ and 5 cm mesh resolutions indicate that the calculated HRR values are slightly overestimated in regard to the ones corresponding to the finest mesh resolutions. The HRR curve corresponding to the 10 cm mesh resolution shows the biggest deviations from the curve corresponding to the finest mesh resolution. These observations indicate that the chosen 2.5 cm mesh resolution can be considered as still fine enough for the intended cinema fire simulation.
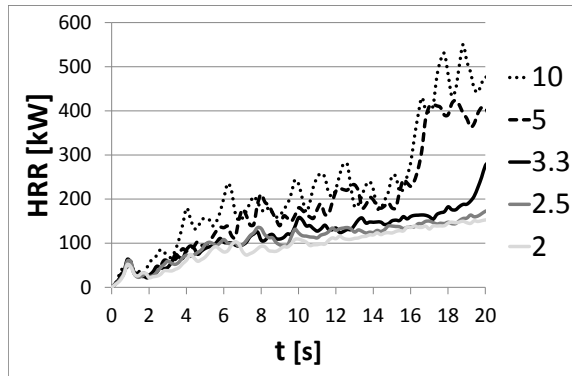

Figure 13. HRR curves corresponding to the auxiliary simulations

Figure 14 illustrates the time curves of the D^*/dx parameter described above, calculated for 5 auxiliary simulations. It follows from the picture that the values of D^*/dx reached the value of 16 at the 5th, 8th and 20th second for the calculation with the 2, 2.5 and $3.\bar{3}$ cm mesh resolution, respectively; however, the calculations with the 5 and 10 cm resolutions did not reach the value of 16 during the first 20 seconds of simulation. Therefore, considering similarity between the types of fire simulated in our 5 auxiliary calculations and those reported in [12], it can be deduced that the flow field in the simulation realised using the 2 and 2.5 cm resolutions is well resolved and the used meshes can be considered as fine enough. Finally, considering the correspondence between the analysed auxiliary simulations and the intended simulation of the cinema hall fire, we can conclude that the 2.5 cm resolution used in the intended simulation can also be considered fine enough. Values of the D^*/dx parameter for the cinema hall fire simulation are illustrated in Figure 15.
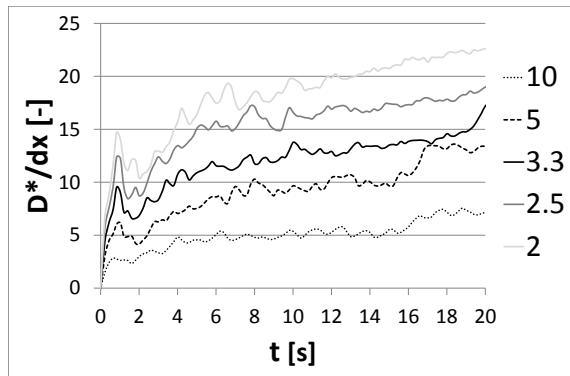

Figure 14. Values of D^*/dx for the auxiliary simulations

For a given mesh resolution, there are two a posteriori mesh quality metrics in FDS that indicate errors in the velocity and scalar fields calculated by LES. LES is a technique to model the dissipative processes that occur at length scales smaller than those that are explicitly solved on the numerical grid (sub-grid scale). These measures model the fraction of unresolved kinetic energy and the fraction of unresolved scalar energy fluctuations at given place and time.

The first metric (the measure of turbulence resolution, denoted by MTR) is a scalar quantity locally defined as [21, 1]

$$MTR(x, y, z; t) = \frac{k_{sgs}}{k_{res} + k_{sgs}}$$

where $k_{res} = \frac{1}{2}\tilde{u}_i\tilde{u}_i$ is the resolved kinetic energy per unit mass, $k_{sgs} = \frac{1}{2}(\tilde{u}_i - \hat{\tilde{u}}_i)^2$ is the sub-grid kinetic energy, $\tilde{u}_i$ is the resolved LES velocity and $\hat{\tilde{u}}$ is test filtered at a scale 2Δ where Δ is the LES filter width (in FDS, $\Delta = dx$). The model for the
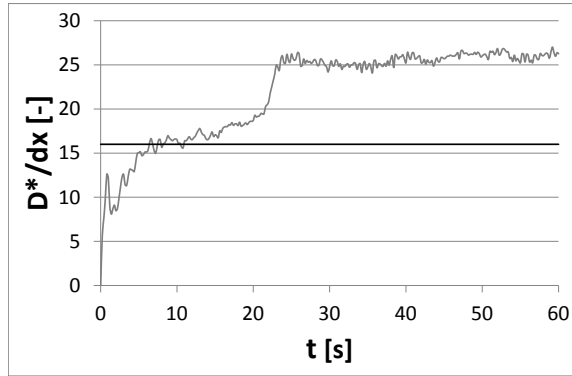
Figure 15. Values of D^*/dx for cinema hall fire simulation (2.5 cm mesh resolution)

sub-grid scale fluctuations is taken from scale similarity [1] and the cross-term energy is ignored. The measure provides the user with an approximation to the Pope criterion [27] and its visualization in a specified plane. The measure falls within the range $[0, 1]$, with 0 indicating perfect resolution and 1 indicating poor resolution (the flow is under-resolved). As shown in [19], maintaining the MTR values near 0.2 provides satisfactory results (simulation results within experimental error bounds) for mean velocities and species concentrations in non-reacting, buoyant plumes. In Figure 16, slices of the MTR values passing through the centre of the fire source in a given time calculated for selected auxiliary simulations using different mesh resolutions are illustrated. It can be seen in Figure 16 that the areas of the maximal reached MTR value in the slice corresponding to the simulation calculated using a coarser (10 cm) mesh resolution are significantly greater than the ones corresponding to the simulations calculated using 2 and 2.5 cm mesh resolutions (fine meshes).
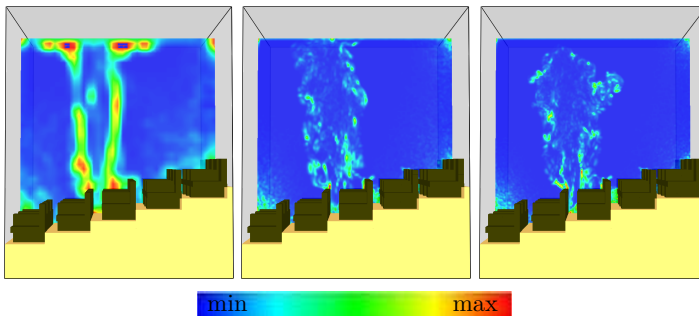

Figure 16. Illustration of the MTR measure at the 4th second for the 10 cm 2.5 cm and 2 cm mesh resolution. The colour scheme values for the 10 cm, and 2.5 cm and 2 cm resolution vary from 0 (blue) to 0.5 (red), and 0 (blue) to 0.45 (red), respectively.

The second metric (the measure of scalar resolution denoted by MSR) is defined locally as [21, 39]

$$MSR(x, y, z; t) = \frac{T_{sgs}}{T_{res} + T_{sgs}}$$

where $T_{res} = \tilde{\varphi}$ and $T_{sgs} = (\tilde{\varphi} - \hat{\tilde{\varphi}})^2$, the model for the sub-grid scale scalar energy fluctuations is taken again from scale similarity [1]; the scalar field $\hat{\tilde{\varphi}}$ is test filtered at a scale 2Δ. The best advice is to keep the MSR values less than 0.2 [21]. In Figure 17, slices of the MSR values passing through the centre of the fire source in a given time calculated for selected auxiliary simulations using different mesh resolutions are illustrated. It can be observed in the figure that the areas of the maximal reached MSR value in the slice corresponding to the simulation calculated using a coarser (10 cm) mesh resolution are significantly greater than those corresponding to the simulations calculated using 2 and 2.5 cm mesh resolutions (fine meshes).
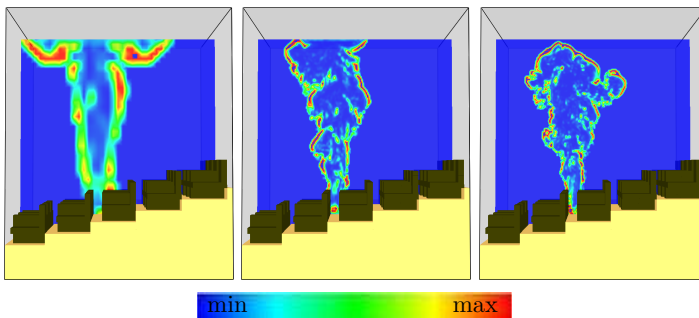

Figure 17. Illustration of the MSR measure at the 4th second for the 10 cm, 2.5 cm and 2 cm mesh resolutions: the colour scheme values for the 10 cm, and 2.5 cm and 2 cm resolution vary from 0 (blue) to 0.65 (red), and 0 (blue) to 0.5 (red), respectively

4.3 Comparison of Parallel to Sequential Calculation

As it was described above, we realised the sequential (1M) and parallel MPI (6M) simulation of the cinema hall fire which used one and 6 CPU cores, respectively. The total computation time of 1M and 6M was 1 890 177.11 s (525.05 hrs) and 331 153.24 s (91.99 hrs), respectively.

Comparison of 6M to 1M in regard of the total computation time is shown in Table 4. In order to show efficiency of the considered parallelization of 1M, we used two standard measures; the speedup $S = T_{1M}/T_{6M}$, where T_{1M} is the total computational time of 1M and T_{6M} is the total computational time of 6M, and the parallel efficiency $E = (S/n) * 100\%$, where n is the number of CPU cores used by parallel calculation. The measure S represents the ability of parallel realization of a computation to decrease the total computation time of the calculation and the measure E refers to the utilization of the CPU cores assigned to the corresponding

Calculation	N_P	N_{MPI}	N_C	t_T [hrs]	S	E [%]
1M	1	–	1	525.05	–	–
6M	–	6	6	91.99	5.71	95

Table 4. Comparison of sequential (1M) and parallel (6M) calculation in regard of total computation time and efficiency of parallelization: N_P is the number of computational processes, N_{MPI} is the number of MPI processes, N_C is the number of CPU cores, t_T is the total computation time, S is the speedup and E is the parallel efficiency

parallel computation. Note that E is a relative quantity given in %, representing the speedup normalized by the number of CPU cores used in parallel calculation which indicates quality of parallelization. Table 4 indicates that the parallelization of 1M using 6 CPU cores accelerated the 1M calculation 5.71 times. The 6M calculation reached the 95 % parallel efficiency. These results indicate that in the case of using relatively small number of CPU cores the time consumed by communication between individual MPI processes did not represent significant part of the total computational time.

In the rest of the paper, we focus on the comparison of 6M to 1M in regard of the simulation accuracy. The sequential calculation 1M is considered as an exact calculation.

	C	L	B	F	R
$t_{\bullet}^{1M}$ [s]	4.0	4.2	7.4	10.4	12.8
$t_{\bullet}^{6M}$ [s]	3.8	4.2	7.2	10.6	13.4
D [s]	0.2	0.0	0.2	0.2	0.6
RD [%]	5	0	3	2	5

Table 5. Comparison of fire behaviours obtained by 1M and 6M: C, B, F, L and R represent the times in which smoke reached the ceiling, the back and front walls, and the left and right curved parts of the ceiling of the cinema hall, respectively; the symbol $\bullet$ means the part of the cinema hall reached by the smoke; and $t_{\bullet}^{1M}$, $t_{\bullet}^{6M}$, D and RD correspond to the times in which smoke hit the corresponding place at the cinema hall in 1M and 6M, the difference $D = \mid t_{\bullet}^{1M} - t_{\bullet}^{6M} \mid$ and the relative difference $RD = (D/t_{\bullet}^{1M}) * 100 \%$, respectively

In order to illustrate inaccuracy in simulation results introduced into the calculation by its parallelization, we compare the simulation results obtained by 1M and 6M. First, we analysed times in which some selected phenomena occurred and could be observed in the fire behaviour. In Table 5 the times in which smoke reached the ceiling, the back and front walls, and the left and right curved parts of the ceiling of the cinema hall are listed. In addition, the table shows the absolute and relative differences between the times considered for the sequential and parallel calculations. It can be seen that the greatest value of D (0.6 s) corresponds to the right curved part of the ceiling. The difference could be caused by the used parallel MPI model of parallelization of 1M. We have pointed out on

possible sources of inaccuracies in parallel MPI FDS simulations in our previous research [41, 10, 42]. Since the computational domain is decomposed into 6 computational meshes on which individual MPI processes that communicate to each other via MPI are realized, the communication between MPI processes (exchange of information between individual MPI processes) causes a loss of information at places where the meshes touch (at the corresponding mesh boundaries). In some cases, during the realization of simulations with a large number of computational meshes, significant inaccuracies in simulation results can appear. On the other hand, the value of RD corresponding to the right curved part of the ceiling is the same as the RD value at the beginning of fire after the smoke hit on the ceiling (5 %). A relatively high value of RD at the 4th second of fire could be caused by uncertainties associated with the beginning of fire development and by relatively high speed of hot gases released from the fire moving towards the ceiling. However, the values of D and RD are still not significant. Table 5 shows that the D and RD values corresponding to the considered times do not exceed the value of 1 s and 5 %, respectively.
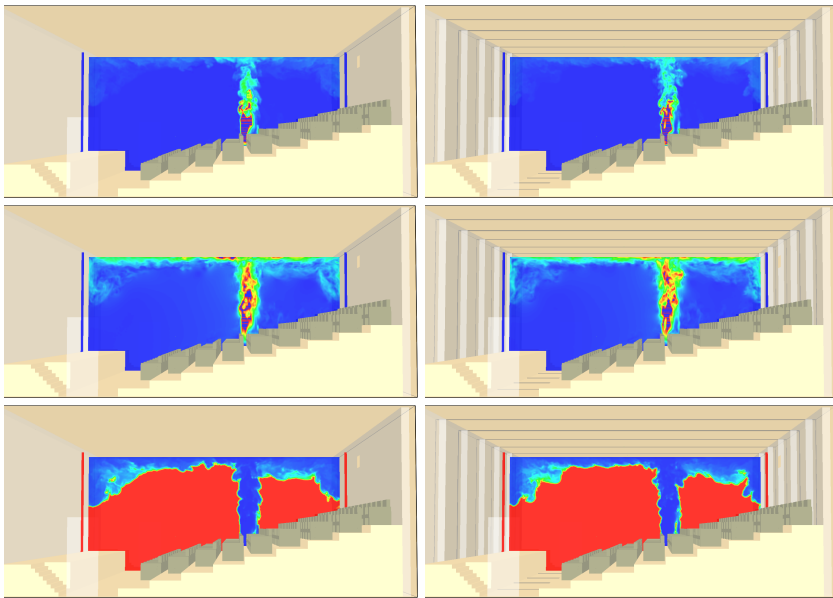

Figure 18. Visualization of temperature, velocity and soot visibility fields corresponding to sequential (left) and parallel (right) calculation at the 20th second

The results of simulation of the temperature, velocity and soot visibility obtained by 1M and 6M are illustrated in Figure 18. There are some differences that can be seen in the figure, however, the main tendencies of the fire behaviour and observed specific phenomena are maintained in the parallel calculation.

Figure 19 shows the time curves of HRR for 1M and 6M. The values of HRR for the particular calculations are slightly different, however, qualitative course of HRR corresponding to both calculations is similar. Thus, we can conclude that parallelization by the parallel MPI model of FDS which uses 6 CPU cores does not cause any significant qualitative errors in HRR evolution during the first minute of the fire.
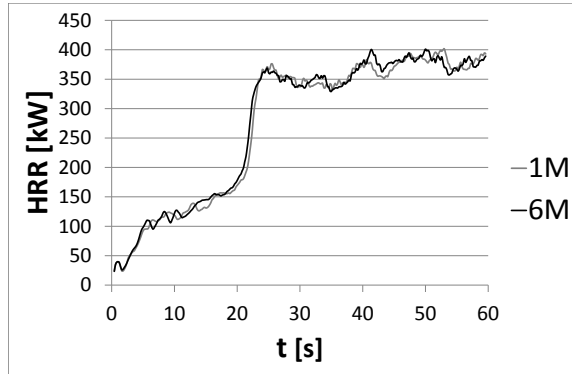

Figure 19. Time curve of HRR for 1M and 6M (5-point moving average)

5 CONCLUSION

This study focused primarily on selected issues related to realization of the simulation of 1-minute lasting fire in small cinema hall with curved ceiling and sloping floor furnished by 108 upholstered chairs which was modelled by the FDS fire simulator. The simulation results confirmed capability of FDS to provide reliable simulations of smoke spread and to capture and visualize specific phenomena appearing during the cinema hall fire. The safety threats for spectators sitting or standing at different places at the cinema hall were indicated. Significant contribution of the curved ceiling and sloping floor to the increase of safety risks to sitting or escaping people even during the first minute of the fire was illustrated. As upholstery is known to produce a huge amount of dense and toxic smoke, the analysis focused rather on the spread of smoke released from upholstered seats fire than on the temperature increase. Material parameters of upholstery considered in the simulation were validated by full-scale upholstered chair fire experiments and by FDS simulation, and determined by laboratory measurements [11].

The paper concentrates on selected issues related to accuracy of the realized simulation, particularly on the mesh sensitivity study and illustration of the impact of the chosen mesh resolution on resolving the velocity and scalar fields calculated. In order to analyse the impact of the mesh resolution on accuracy of the compu-

tation, five auxiliary simulations were realised in which the corresponding part of the cinema hall was used. These simulations were used for the purpose of the mesh sensitivity study and visualization of two measures indicating the errors in the velocity and scalar fields calculated by LES. The analysis confirmed that the chosen computational meshes with the 2.5 cm resolution can be considered fine enough for the intended cinema hall fire simulation.

The sequential calculation 1M using one CPU core and the parallel MPI calculation 6M using 6 CPU cores with the computational domain decomposed into 6 computational meshes with the same mesh resolution were realised.

In order to show the efficiency of the considered parallelization, the speedup and the parallel efficiency were calculated. The results obtained showed that the parallel MPI calculation using 6 CPU cores accelerated the 1M calculation 5.71 times and reached the 95 % parallel efficiency. These results indicate that the use of relatively small number of cores leads to high acceleration of computation and the time consumed for communication between individual MPI processes is not significant. However, future research is necessary to show the relation between the number of used CPU cores and the total computation time for large numbers of meshes.

In order to illustrate the simulation inaccuracy caused by parallelization, the times of selected phenomena occurrence in the fire behaviour were analysed. Hits of smoke onto the ceiling, the back and front walls, and the left and right curved parts of the ceiling of the cinema hall were recorded and the absolute and relative differences between the times considered for the sequential and parallel calculations were analysed. Values of the absolute and relative difference obtained did not exceed value of 1 s and 5 %, respectively.

Differences in the gas temperature, velocity, soot visibility and HRR obtained by 1M and 6M were also discussed. Small differences, but maintaining the main tendencies of the fire behaviour and occurred specific phenomena were observed indicating that the parallelization using 6 CPU cores does not cause any significant qualitative errors in considered quantities at considered times. However, further research is required to study inaccuracies involved by parallelization in the case of large number of meshes. The results of this study also indicate the need of further investigation of other important aspects of realization of the cinema hall fire simulation related to fires in large complex structures (e.g. with several cinema or multi-purpose halls). Proper parallelization of such calculations must be considered and carefully analysed. Other challenging issue is the study of relation between efficiency and accuracy of such calculations realised on HPC clusters.

This study had continued in our previous research on modelling of the fire dynamics and effects of fire in cinema hall (see above) in which the fire source was placed at different positions. This research has confirmed a great potential of FDS for capturing specific tendencies of the fire and smoke spread in such structures and also put in focus that a specific geometry of the structures significantly influences the fire behaviour. Results of this study indicate than proper parallelization of the fire

simulation using FDS can significantly increase efficiency of the calculation without a significant decrease of the calculation accuracy.

Acknowledgement

REFERENCES

[1] BARDINA, J.—FERZIGER, J. H.—REYNOLDS, W. C.: Improved Subgrid Scale Models for Large Eddy Simulation. AIAA 13th Fluid and Plasma Dynamics Conference, AIAA-80-1357, American Institute of Aeronautics and Astronautics, Snowmass, Colorado, July 1980, doi: 10.2514/6.1980-1357.

[2] BUDINSKA, I.—HLUCHY, L.: Distributed Computing and Complex Applications. Computing and Informatics, Vol. 35, 2016, No. 6, pp. 1356–1358.

[3] CHEN, F.—LEONG, J. C.: Smoke Flow Phenomena and Turbulence Characteristics of Tunnel Fires. Applied Mathematics Modelling, Vol. 35, 2011, pp. 4554–4566, doi: 10.1016/j.apm.2011.03.033.

[4] DVORAK, O.—ANGELIS, J.—KUNDRATA, T.—MATHEISLOVA, H.—BURSIKOVA, P.—JAHODA, M.: Computer Simulation of a Fire Test in Mokrsko (in Czech). Transactions of the VSB-TU Ostrava, Vol. 5, 2010, No. 2, pp. 45–52.

[5] FORNEY, G. P.—MOSS, W. F.: Analyzing and Exploiting Numerical Characteristics of Zone Fire Models. Fire Science and Technology, Vol. 14, 1994, No. 1–2, pp. 49–60, doi: 10.3210/fst.14.49.

[6] GLASA, J.—VALASEK, L.: Study of Applicability of FDS+Evac for Evacuation Modeling in Case of Road Tunnel Fire. Research Journal of Applied Sciences, Engineering and Technology, Vol. 7, 2014, No. 17, pp. 3603–3615, doi: 10.19026/rjaset.7.713.

[7] GLASA, J.—VALASEK, L.—HALADA, L.—WEISENPACHER, P.: Impact of Turned Cars in Tunnel on Modelling People Evacuation in Fire Conditions. Proceedings of the 8th EUROSIM Congress on Modelling and Simulation, IEEE Computer Society (CPS), Cardiff, 2014, pp. 84–89.

[8] GLASA, J.—VALASEK, L.—WEISENPACHER, P.—HALADA, L.: Use of PyroSim for Simulation of Cinema Fire. International Journal on Recent Trends in Engineering and Technology, Vol. 7, 2012, No. 2, pp. 51–56.

[9] GLASA, J.—VALASEK, L.—WEISENPACHER, P.—HALADA, L.: Cinema Fire Modelling by FDS. Journal of Physics: Conference Series, Vol. 410, 2013, No. 1, DOI 10.1088/1742-6596/410/1/012013

[10] HALADA, L.—WEISENPACHER, P.—GLASA, J.: Computer Modelling of Automobile Fires (Chapter 9). Liu, Ch. (Ed.): Advances in Modeling of Fluid Dynamics, InTech Publisher, Rijeka, 2012, pp. 203–229.

[11] HIETANIEMI, J.—HOSTIKKA, S.—VAARI, J.: FDS Simulation of Fire Spread – Comparison of Model Results with Experimental Data. VTT Working Papers 1459-7683, VTT Building and Transport, Finland, 2004.

[12] HILL, K.—DREISBACH, J.—JOGLAR, F.—NAJAFI, B.—MCGRATTAN, K.—PEACOCK, R.—HAMINS, A.: Verification and Validation of Selected Fire Models for Nuclear Power Plant Applications. NUREG 1824. United States Nuclear Regulatory Commission, Washington, DC, 2007.

[13] HOROVA, K.—JANA, T.—WALD, F.: Temperature Heterogeneity During Travelling Fire on Experimental Building. Advances in Engineering Software, Vol. 62–63, 2013, pp. 119–130.

[14] HWANG, CH.-H.—LOCK, A.—BUNDY, M.—JOHNSSON, E.—KO, G. H.: Studies on Fire Characteristics in Over- and Underventilated Full-Scale Compartments. Journal of Fire Sciences, Vol. 28, 2010, No. 5, pp. 459–486.

[15] JAHN, W.—REIN, G.—TORERO, J. L.: Forecasting Fire Dynamics Using Inverse Computational Fluid Dynamics and Tangent Linearisation. Advances in Engineering Software, Vol. 47, 2012, No. 1, pp. 114–126.

[16] JONES, W. W.: A Review of Compartment Fire Models. NBSIR 83-2684, National Bureau of Standards (Now NIST), Gaithersburg, Maryland, 1983.

[17] LING, D.—KAN, K.: Numerical Simulations on Fire and Analysis of the Spread Characteristics of Smoke in Supermarket. Communications in Computer and Information Science, Vol. 176, 2011, No. 1, pp. 7–13, doi: 10.1007/978-3-642-21802-6_2.

[18] MATHEISLOVA, H.—JAHODA, M.—KUNDRATA, T.—DVORAK, O.: CFD Simulations of Compartment Fires. Chemical Engineering Transactions, Vol. 21, 2010, pp. 1117–1122, doi: 10.3303/CET1021187.

[19] MCDERMOTT, R. J.—FORNEY, G. P.—MCGRATTAN, K. B.—MELL, W. E.: Fire Dynamics Simulator 6: Complex Geometry, Embedded Meshes, and Quality Assessment. Pereira, J. C. F., Sequeira, A. (Eds.): Fifth European Conference on Computational Fluid Dynamics, Lisbon, Portugal, 2010.

[20] MCGRATTAN, K.—BAUM, H.—REHM, R. —MELL, W.—MCDERMOTT, R.—HOSTIKKA, S.—FLOYD, J.: Fire Dynamics Simulator (Version 5), Technical Reference Guide. NIST Special Publication 1018-5, NIST, Gaithersburg, Maryland, USA, 2010.

[21] MCGRATTAN, K.—KLEIN, B.—HOSTIKKA, S.—FLOYD, J.: Fire Dynamics Simulator (Version 5), User's Guide. NIST Special Publication 1019-5, NIST, Gaithersburg, Maryland, USA, 2009.

[22] MCGRATTAN, K.—MCDERMOTT, R.—FLOYD, J.—HOSTIKKA, S.—FORNEY, G.—BAUM, H.: Computational Fluid Dynamics Modelling of Fire. International Journal of Computational Fluid Dynamics, Vol. 26, 2012, No. 6–8, pp. 349–361, doi: 10.1080/10618562.2012.659663.

[23] MOIN, P.—MAHESH, K.: Direct Numerical Simulation: A Tool in Turbulence Research. Center for Turbulence Research, Stanford University, Stanford, CA 94305 and NASA Ames Research Center, Moffett Field, California, 1998, pp. 539–578.

[24] Open MPI – A High Performance Message Passing Library. Available from: `http://www.open-mpi.org/`.

[25] OpenMP – Open Multi-Processing, API Specification for Parallel Programming. Available from: `http://openmp.org/`.

[26] ORAN, E. S.—BORIS, J. P.: Numerical Simulation of Reactive Flow. Elsevier Science Publishing Company, New York, 1987.

[27] POPE, S. B.: Ten Questions Concerning the Large-Eddy Simulation of Turbulent Flows. New Journal of Physics, Vol. 6, 2004, No. 35, pp. 1-24, doi: 10.1088/1367-2630/6/1/035.

[28] PRASAD, K.—KRAMER, R.—MARSH, N.—NYDEN, M.—OHLEMILLER, T.—ZAMMARANO, M.: Numerical Simulation of Fire Spread on Polyurethane Foam Slabs. Fire Research Division NIST, Gaithersburg, MD, USA, 2009.

[29] QUINTIERE, J.: A Perspective on Compartment Fire Growth. Combustion Science and Technology, Vol. 39, 1984, No. 1–6, pp. 11–54, doi: 10.1080/00102208408923782.

[30] REHM, R. G.—BAUM, H. R.: The Equations of Motion for Thermally Driven, Buoyant Flows. Journal of Research of the NBS, Vol. 83, 1978, No. 3, pp. 297–308.

[31] REIN, G.—BAR-ILAN, A.—FERNANDEZ-PELLO, A. C.—ALVARES, N.: A Comparison of Three Models for the Simulation of Accidental Fires. Journal of Fire Protection Engineering, Vol. 16, 2006, No. 3, pp. 183–209, doi: 10.1177/1042391506056926.

[32] STERN-GOTTFRIED, J.—REIN, G.—BISBY, L. A.—TORERO, J. L.: Experimental Review of the Homogeneous Temperature Assumption in Post-Flashover Compartment Fires. Fire Safety Journal, Vol. 45, 2010, No. 4, pp. 249–261, doi: 10.1016/j.firesaf.2010.03.007.

[33] SWEET, R. A.: Direct Methods for the Solution of Poisson's Equation on a Staggered Grid. Journal of Computational Physics, Vol. 12, 1973, No. 3, pp. 422–428.

[34] THOMAS, I. R.—MOINUDDIN, K. A. M.—BENNETTS, I. D.: The Effect of Fuel Quantity and Location on Small Enclosure Fires. Journal of Fire Protection Engineering, Vol. 17, 2007, No. 2, pp. 85–102, doi: 10.1177/1042391506064908.

[35] Thunderhead Engineering: PyroSim User Manual 2008.1. Thunderhead Engineering, Manhattan, 2008.

[36] VALASEK, L.: The Use of PyroSim for Creation of the Input FDS Geometry for Cinema Fire Simulation. Proceedings of the 3rd European Conference of Systems, Paris, December 2012, pp. 304–309.

[37] VALASEK, L.: The Use of PyroSim Graphical User Interface for FDS Simulation of a Cinema Fire. International Journal of Mathematics and Computers in Simulation, Vol. 7, 2013, No. 3, pp. 258–266.

[38] VALASEK, L.—GLASA, J.—WEISENPACHER, P.—HALADA, L.: Impact of Vehicles on Smoke Spread Dynamics in the Case of Fire in Road Tunnel. Journal of Physics: Conference Series, Vol. 574, 2015, No. 1, doi: 10.1088/1742-6596/574/1/012147.

[39] VERVISCH, L.—DOMINGO, P.—LODATO, G.—VEYNANTE, D.: Scalar Energy Fluctuations in Large-Eddy Simulation of Turbulent Flames: Statistical Budgets and Mesh Quality Criterion. Combustion and Flame, Vol. 157, 2010, No. 4, pp. 778–789, doi: 10.1016/j.combustflame.2009.12.017.

[40] WANG, M. Y.—HAN, X.—WU, G. H.—LIU, Q. Q.: Simulation Analysis of Temperature Characteristics for a Theater Fire. Proceedings of the International Symposium on Innovations and Sustainability of Structures in Civil Engineering, Vol. 1–2, Shanghai, PR China, 2008, pp. 1145–1152.

[41] WEISENPACHER, P.—GLASA, J.—HALADA, L.—VALASEK, L.—SIPKOVA, V.: Parallel Computer Simulation of Fire in Road Tunnel and People Evacuation. Computing and Informatics, Vol. 33, 2014, No. 6, pp. 1237–1268.

[42] WEISENPACHER, P.—HALADA, L.—GLASA, J.—ASTALOS, J.: Influence of Parked Cars on Smoke Propagation During Car Park Fire. Proceedings of the 26th European Modeling and Simulation Symposium, Bordeaux, DIME Universita di Genova, 2014, pp. 384–391.

[43] WEISENPACHER, P.—GLASA, J.—HALADA, L.: Parallel Computation of Smoke Movement During a Car Park Fire. Computing and Informatics, Vol. 35, 2016, No. 6, pp. 1416–1437.

[44] WU, G. H.—HAN, X.—WANG, M. Y.—LIU, Q.: Simulation Analysis of Smoke Distribution Features for a Theater Fire. Proceedings of the International Symposium on Innovations and Sustainability of Structures in Civil Engineering, Vol. 1–2, Shanghai, PR China, 2008, pp. 1153–1159.

[45] ZHANG, X.—YANG, M.—WANG, J.—HE, Y.: Effects of Computational Domain on Numerical Simulation of Building Fires. Journal of Fire Protection Engineering, Vol. 20, 2010, No. 4, pp. 225–251.

[46] ZOU, G. W.—CHOW, W. K.: Evaluation of the Field Model, Fire Dynamics Simulator, for a Specific Experimental Scenario. Journal of Fire Protection Engineering, Vol. 15, 2005, No. 2, pp. 77–92.

Lukáš VALÁŠEK graduated in applied mathematics in 2012, received his Eng. degree in mathematical and computer modelling at the Slovak University of Technology in Bratislava, Faculty of Civil Engineering and his Ph.D. degree in applied informatics at the Slovak University of Technology in Bratislava, Faculty of Informatics and Information Technologies. He works for the Institute of Informatics, Slovak Academy of Sciences in Bratislava. His major research interests include mathematical modelling and computer simulation of fires and their consequences.

Jan GLASA graduated in numerical mathematics in 1986, received his R.N.Dr. (Rerum Naturalium Doctor) degree in numerical mathematics and optimization methods and algorithms at the Comenius University in Bratislava, Slovakia and his C.Sc. degree (equivalent to Ph.D.) in computer science at the Slovak Academy of Sciences. He works for the Institute of Informatics, Slovak Academy of Sciences in Bratislava as Senior Scientist and serves as the head of the Scientific Council of the Institute. His current research interests include mathematical modelling and computer simulation of fires and parallel computing.